A short review of Precambrian and Phanerozoic sedimentary iron (± Mn, P) ore deposits

Review and explanatory notes of photographs by Andreas G. Mueller, 12a Belgrave Street, Maylands W.A. 6051, Australia
E-mail: andreasm@iinet.net.au

July 2019

Contents

1. Technical aspects and copyright

The images stored in folders are high-quality (200 dpi) JPEG-files saved with the color profile "Adobe RGB 1998". The Adobe color space has a broader range than the older "sRGB IEC6-1966-2.1" profile. The Microsoft and Apple operating systems allow selection of the color profile for the display screen in the "System Preferences" under "Displays". The embedded color of each photograph can be changed in Adobe Photoshop Creative Suite (CS) and in Adobe Photoshop Elements, computer programs available at most universities. The author releases the images and these explanatory notes for teaching purposes at universities and other public institutions. The photographs are available as free downloads from the SGA website (e-sga.org, Publications, Archive). They are signed "AGM + year" by the author, who retains the copyright. The copyright cannot be transferred to a journal, publisher or any media organization without written consent. The photographs are intended to remain free-of-charge Open Access indefinitely. Acknowledgements should be made to the author and to the SGA website in the customary way. The text below has been carefully edited and was reviewed by Carlos Alberto Rosière, who contributed the photographs from the Quadrilátero Ferrífero in Minas Gerais, Brazil.

2. Introduction

The photographs described and the references quoted may serve as a brief introduction to the geology of Precambrian banded iron formations (BIFs), the main source of iron ore today, and to the geology of Mesozoic ironstones in Europe, the main source of iron during the industrial revolution in the 19th century. This overview is not comprehensive and limited to locations visited by the author. The reader is referred to the Special Issue in Economic Geology 1973 (no. 7) on Precambrian iron formations, which includes reviews of deposits

in the United States (Lake Superior), Canada (Algoma), Australia (Hamersley), South Africa (Transvaal), Brazil (Minas Gerais) and the former Soviet Union (Krivoy Rog). A recent review of this deposit class is in the 100th Anniversary Volume of Economic Geology (Clout and Simonson 2005; pp. 643-679).

In his classic paper, James (1954) subdivided the banded iron formations of the Lake Superior region into oxide, carbonate, silicate and sulfide sedimentary facies. Klein (2005) provides an excellent overview of depositional mechanisms, mineralogical changes with metamorphic grade, and periods of BIF deposition during the Earth's history. The most productive period is the Early Proterozoic, related to the "Great Oxidation Event" at 2.5-2.4 Ga when the atmosphere-hydrosphere system evolved from anoxic to oxidizing conditions due to photosynthetic activity (Krupp et al. 1994; Holland 2005).

The great iron ore mines in marine oolitic ironstones in Europe were closed during the 1970s and early 1980s due to lower grades (30-40% Fe) relative to the BIF-hosted enriched ore bodies (>60% Fe) mined overseas. The deposits are still of interest given well-studied sedimentary facies relations and the lack of metamorphic overprint. A useful review, though dated, is in the textbook of Beyschlag, Vogt and Krusch (1914, pp. 979-1114) in its English translation, which includes a section on sedimentary manganese deposits. Another source are the reviews in the series "Mineral deposits of Europe" (1978-1986) issued by the Institution of Mining and Metallurgy London on ironstone deposits in the United Kingdom, Germany and France. Explanatory notes and tables accompany the International Map of the Iron Ore Deposits of Europe 1:2,500,000 published by the Federal Geological Survey of Germany (BGR 1977, 1978).

Some Precambrian banded iron formations also contain large (>100 million tons) manganese deposits, and Mesozoic-Cenozoic oolitic manganese deposits of similar size are mined on Groote Eylandt, Australia, and at the periphery of the Black Sea, east Europe (Laznicka 1992). Several Mn-deposits and genetic aspects are reviewed in the Economic Geology Special Issue on manganese metallogenesis (1992, vol. 87, no. 5). Below, key deposits are briefly referred to in the context of genetically related iron ore. The transport of divalent Fe and Mn in solution, and the precipitation of both metals as silica gels or carbonate under reducing or as insoluble oxides under oxidizing conditions are covered in Roy (2006), Maynard (2010), and the reviews introduced above.

3. Archean Algoma-type iron formations

The oldest known Archean iron formation occurs in the 3.77 Ga Isua supracrustal belt, West Greenland (e.g. Czaja et al. 2013). In Canada, Archean BIFs have been subdivided into the "geosynclinal" Algoma-type associated with volcanic successions in greenstone belts, and into the "platform" Superior-type associated with shelf quartzites and dolomites (Gross 1980). In the Abitibi greenstone belt, oxide-facies quartz-magnetite iron formation in Quebec extends 36 km in strike, is 120-600 m thick, and contains a low-grade resource of 3.7 billion metric tons at 22.2 % iron (Taner and Chemam 2015). BIF in the Helen Range of the Michipicoten greenstone belt is the type locality for Algoma-type carbonate facies. Thick-bedded siderite with intercalated beds of granular silica, graphitic argillite and syngenetic pyrite + pyrrhotite is overlain by quartz-siderite-magnetite BIF mesobanded on a mm- to cm-scale (Fig. 1). The siderite ore body at the MacLeod mine is 2 km long, 60-150 m thick, averages 35 wt.% Fe and 3.9% S, and contains >100 million tons of ore (Goodwin 1964). Stromatolites preserved in the uppermost part of the siderite unit indicate deposition at low temperature (<110°C) in shallow water (Hofmann et al. 1991). The stromatolites support the facies model of Klein (2005) placing oxide BIF into the deeper part of the sedimentary basin proximal to hydrothermal vents, and black shale, sulfide and siderite BIF into the shallow parts influenced by the anoxic Archean atmosphere.

In the Archean Yilgarn craton of Western Australia, Algoma-type banded iron formation forms a distinctive marker horizon in the 3.0 Ga ultramafic-mafic volcanic succession of the Marda, Southern Cross and Koolyanobbing greenstone belts (Gole 1981) located in the Mesoarchean continental foreland of the 2.7 Ga Eastern Goldfields orogen.
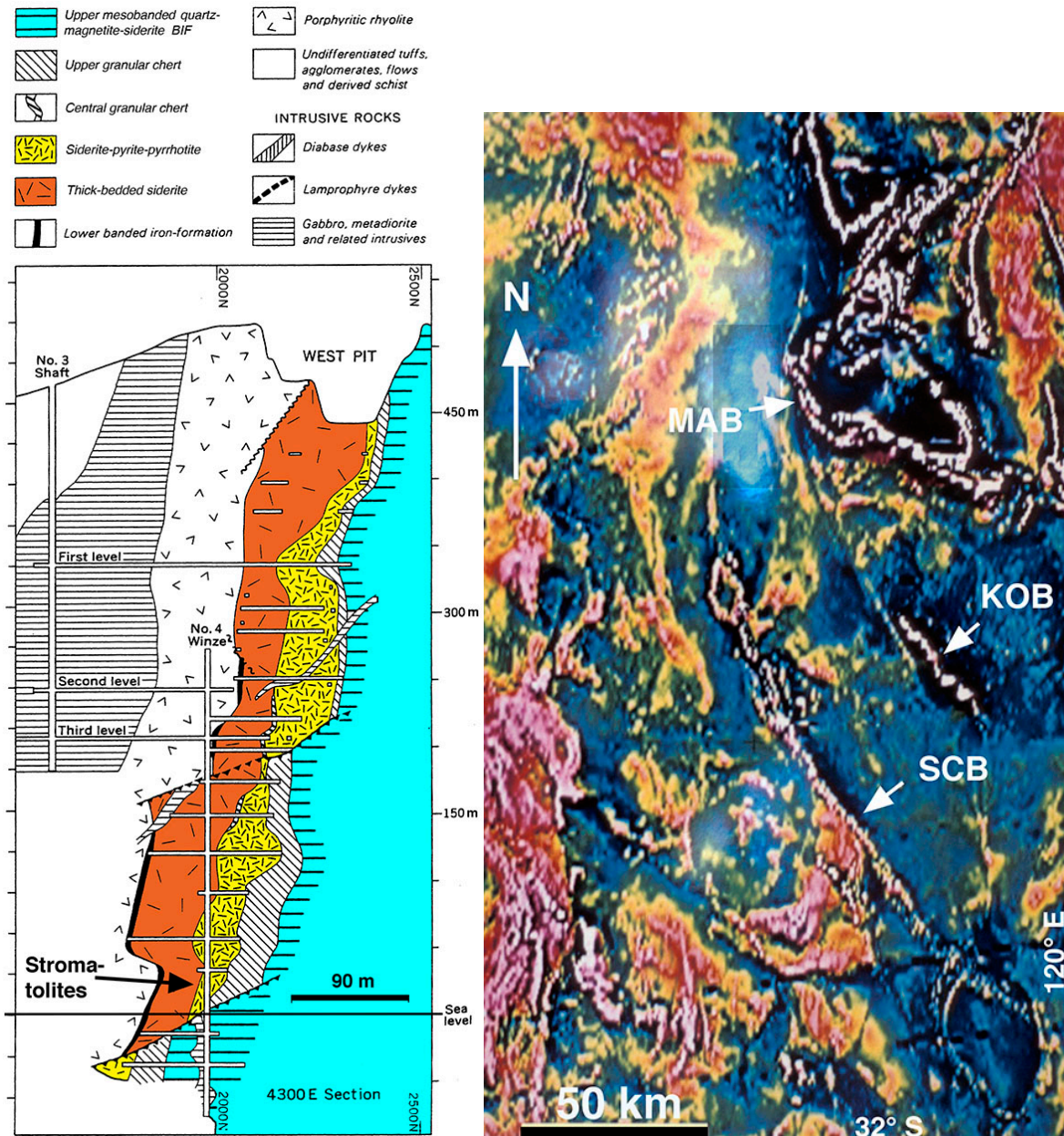
Figure 1: Algoma-type banded iron-formation. LEFT: Cross section through the siderite-sulfide iron formation of the Helen mine, Michipicoten greenstone belt, Canada (modified from Douglas 1970). The location of the stromatolites is shown schematically, as they were found in the deeper part of the ore body, MacLeod mine. RIGHT: Total magnetic intensity map of the central Yilgarn Craton, Western Australia, showing the folded banded iron-formation marker horizon (white pixelated lines) in the 3.0 Ga old Marda (MAB), Koolyanobbing (KOB) and Southern Cross (SCB) greenstones belts (black-blue) separated by orthogneiss and magnetite-series granite batholiths (modified from the Perth 1:1000,000 TMI map sheet, Australian Geological Survey Organisation1997).

The BIF marker horizon persists for >100 km and allows stratigraphic correlation between greenstone belts separated by granite batholiths (Fig. 1). The metamorphic grade varies from low (prehnite-pumpellyite, greenschist) in the central parts of the wider belts to high (amphibolite, granulite) in 1-2 km wide aureoles surrounding the batholiths. High-grade metamorphic pyroxene-fayalite assemblages in silicate-facies BIF indicate peak temperatures of 670±50°C and pressures of 3-5 kbar in parts of the Southern Cross Belt (Gole and Klein 1981).

The depositional facies in the BIF horizon, mostly 2-3 beds separated by intercalated mafic-ultramafic volcanic rocks, varies from mainly oxide (quartz-magnetite) in the Marda

Belt to mainly silicate (grunerite-magnetite ± quartz) in the Southern Cross Belt. In the Koolyanobbing Belt, much of the BIF horizon is at greenschist metamorphic grade indicated by intercalated chlorite schist, and talc-minnesotaite and siderite mesobands. The grade increases in the 1-2 km wide contact metamorphic aureole rimming the belt where amphiboles of the cummingtonite-grunerite series predominate (Griffin 1981). The origin of the siderite and talc-minesotaite mesobands is controversial. Both minerals may be interpreted as low-grade metamorphic (Klein 2005) or as hydrothermal replacement (Angerer and Hagemann 2010; Angerer et al. 2012).

The Koolyanobbing Belt contains the several high-grade (>58 wt% Fe) iron ore deposits labeled A to F with a total combined pre-mining resource of about 150 million tons, the largest in the Yilgarn Craton (Angerer and Hagemann 2010). In the K-deposit (Dowd's Hill; 100 Mt), specular hematite ore is associated with hydrothermal breccia between two NNE-striking dextral strike-slip faults. In the A deposit, deep laterite weathering formed limonitic goethite ore on siderite-magnetite and pyrite BIF. The petrographic similarity between the A-deposit siderite-magnetite-pyrite BIF and the Helen Range type locality in Canada suggests that the Koolyanobbing siderite BIF is primary carbonate facies at low metamorphic grade. The mesobanded talc-minnesotaite-magnetite BIF in the K-deposit may represent primary silicate facies, the precursor to cummingtonite-grunerite-magnetite BIF at higher metamorphic grade in the Southern Cross Belt.

Photograph YilgarnMardaBIF: Oxide-facies BIF, greenschist metamorphic grade, Marda Belt, Evanston gold mine, Mt Jackson, Western Australia. Algoma-type quartz-magnetite banded iron-formation, 3.0 Ga Diemals-Marda greenstone belt, central Yilgarn Craton. Note the rootless folds in some mesobands. The scale is in centimeters.

Photographs YilgarnSthCrossBIF1 and BIF2: Oxide-facies BIF, amphibolite metamorphic grade, Southern Cross Belt, Lake Koorkoordine north of Southern Cross town: Weathered, leached banded iron formation, outcrops occur over a width of 15-20 m forming a hard ridge at UTM 6546548 m N, 718399 m E (WGS 1984, Zone 50J). The BIF has an overall strike of N40°W and an average dip of about 70°SW. It is non-magnetic and mesobanded on a 1-20 mm scale. Grey mesobands of chert are separated by thinner ones of dark brown goethite after primary magnetite. Rare beds of light green amphibole-chlorite rock up to 2 cm thick are intercalated. The mesobands display abundant intrafolial folds on a decimeter-scale in sections perpendicular to both strike and dip. These folds contrast with the straight lithological contacts of the BIF horizon. They are internal and without significance for the large-scale fold structure. Thin white quartz veins are mostly sub-parallel to mesobands. The pen is 14 cm long.

Photograph YilgarnSthCrossBIF3: Oxide- and silicate-facies BIF, Southern Cross Belt. The matchstick is 4 cm long. LEFT: Oxide-facies BIF, amphibolite metamorphic grade, outcrop at the pipeline memorial about 100 m north of the Great Eastern Highway at the west end of Southern Cross town. The sample is magnetic, and composed of 0.5-3 mm thick dark grey mesobands of cherty quartz (hard > steel) fractured perpendicular to the banding, which alternate with light blue-grey mesobands of magnetite partly weathered to hematite. Brown limonite lines fractures. The iron-oxide bands are fragmented, probably due to slip on quartz mesobands. Iron silicates are absent.

RIGHT: Silicate-facies BIF, amphibolite to granulite metamorphic grade, Mt Palmer gold mine, outcrop of banded iron formation (BIF) on the ridge close to the playa lake. Magnetite-grunerite iron formation banded on a 0.5-8 mm scale, about 60 vol.% magnetite and 40% grunerite in mesobands. Part of the cut specimen contains an 8 mm wide band of coarser-grained (2-5 mm) pyroxene tarnished to the same light brown as grunerite. There is also an accessory (2-3%) dark brown granular mineral (1 mm) rimmed by limonite forming microbands in contact with grunerite mesobands, perhaps fayalite. Pyroxene and fayalite (?) fill a 2 mm thick veinlet crossing the mesobands. Mt Palmer is close to the locations sampled by Gole and Klein (1981), who determined metamorphic conditions of 670 ± 50°C and 3-5 kbar in the aureole of the Ghooli Dome granite batholith.

Photograph YilgarnSthCrossBIF4: Silicate-facies BIF, amphibolite metamorphic grade, Southern Cross Belt, Nevoria gold mine (latitude 31°31' south, longitude 119°35' east), waste-rock dump of the Kurrajong open pit, least-altered iron formation, weakly oxidized, mesobanded on a 0.5-3 mm scale. About 50 vol.% tarnished light yellow-brown grunerite (0.5-1 mm) mesobands, 40 vol.% dark grey granular quartz mesobands, and 5 % black magnetite (magnetic) in spaced meso- and microbands. The brown goethite vein probably represents oxidized gold-related pyrrhotite. The matchstick is 42 mm long.

Photograph YilgarnSthCrossBIF5: Silicate-facies BIF, amphibolite metamorphic grade, Southern Cross Belt, Nevoria gold skarn deposit, drill hole DDH-2, 103.0 m: Unaltered quartz-grunerite iron formation, bands of light brown randomly oriented grunerite (lamellar twins) alternate with bands of clear polygonal quartz, minor opaque magnetite, plane polarized transmitted light, the field of view is 3.4 mm wide.

Photograph YilgarnKoolSdBIF: Carbonate-facies BIF, greenschist metamorphic grade, Koolyanobbing greenstone belt, F-deposit siderite-magnetite BIF, drill hole DDF-2, 141.5 m. Mesobanded black to light brown, fine-grained (0.1-0.5 mm) iron formation, 0.5-8 mm thick mesobands. The black magnetite bands (strongly magnetic) are fractured, and contain minor interstitial chlorite and carbonate. The light brown siderite bands enclose magnetite microbands. Some siderite is partly recrystallized to lenses of coarser grain. The mesobands are cut by a discontinuous, 2 mm-thick brown siderite vein (soft) containing 3 % brass-yellow pyrite (0.5-1 mm), and rare red hematite spots at siderite grain boundaries. X-ray diffraction analysis: Magnetite major, siderite major, quartz rare, chlorite rare. The visible part of the matchstick is 3 cm long, the drill core 4 cm wide.

The **Weld Range** is part of the Meekatharra-Mt Magnet greenstone belt NNW of the Southern Cross Belt, also in the Mesoarchean part of the Yilgarn craton. The range contains oxide, silicate and carbonate facies banded iron formations and iron shales of low metamorphic grade (320±50°C) characterized by greenalite, chamosite, minnesotaite, and siderite (Gole 1980). Minnesotaite is widespread in mesobands alternating with magnetite mesobands. Textures indicate the replacement of quartz-siderite, quartz-greenalite, and greenalite-quartz-siderite assemblages by minnesotaite (Gole 1980).

Gole (1980) interprets the BIF-assemblages as low-grade metamorphic, equivalent to those described from well-studied Proterozoic iron formations (Floran and Papike 1978). In contrast, Duuring and Hagemann (2013) interpret siderite as a hydrothermal mineral selectively replacing quartz mesobands. Two high-grade iron ore deposits (>55 wt.% Fe) in the Beebyn (62 Mt) and Madoonga (68 Mt) BIFs are interpreted to result from the residual enrichment of magnetite due to the leaching of siderite.

Photograph YilgarnWeldRgBIF: Oxide-facies BIF, low metamorphic grade (prehnite-pumpellyite or greenschist facies), Weld Range, Yilgarn Craton, Western Australia. Hematite-rich chert banded red and grey, weakly magnetic, sample from prospect W15, an outcrop a short distance west of the main highway transecting the Weld Range. The Australian 1 Dollar coin is 25 mm across.

4. Proterozoic Lake Superior iron formations, Minnesota-Michigan, USA

The Lake Superior region is the type locality for iron formations deposited together with conglomerate, quartzite and carbonate beds on the shelf of Archean cratons during and after the Great Oxidation of the Earth's atmosphere and hydrosphere at ca. 2.4 Ga. This is the area where James (1954) developed his sedimentary facies model, and where Floran and Papike (1978) described the mineralogical changes and reactions with increasing metamorphic grade in the greenalite, minnesotaite, grunerite and ferrohypersthene zones of the Gunflint Formation, both landmark studies. Reviews of the Lake Superior iron ore district (Fig. 2) are in Lindgren's textbook (1933) and in the Graton-Sales Volume 1: Ore Deposits of the United States 1933-1967, p. 489-549 (American Inst Min Metall Petrol Eng, New York, 1968). Past production from the Lake Superior district is 5.1 billion metric tons (1854-1990) compared to 3.7 billion tons from Krivoi Rog, Ukraine (Machamer et al. 1991).
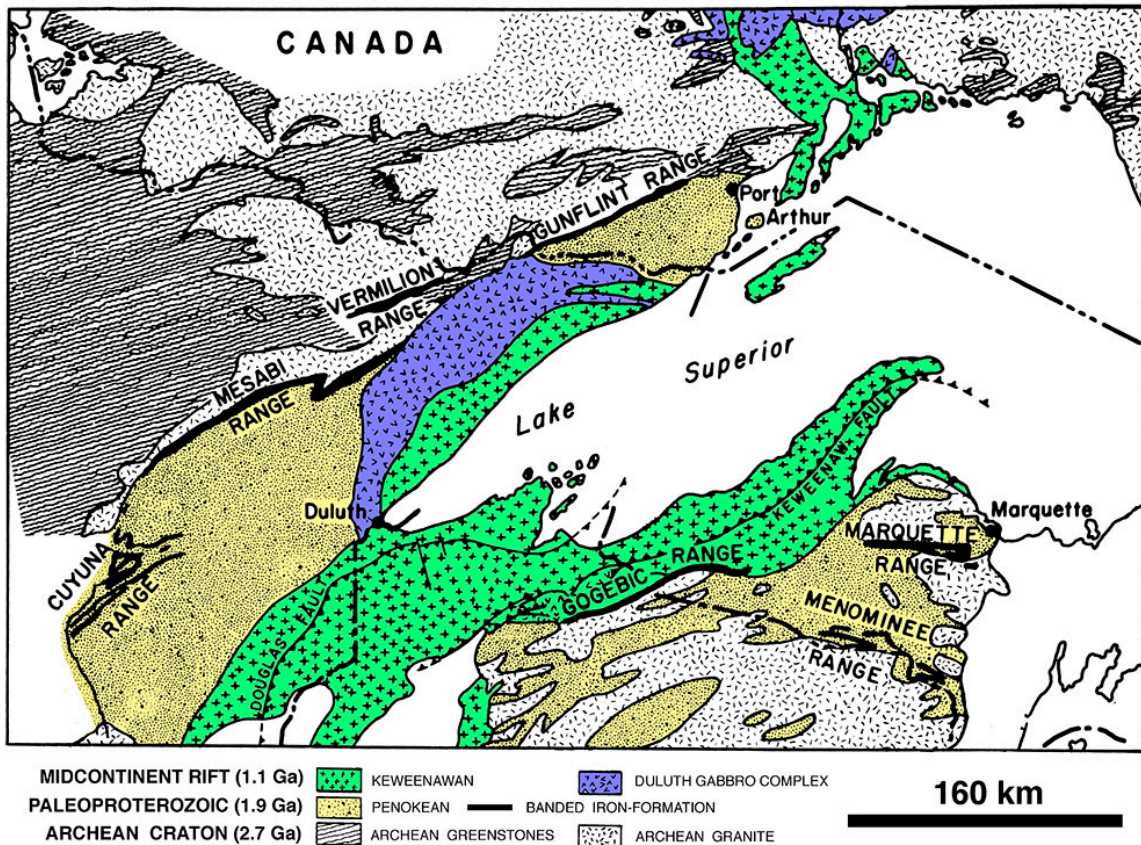
Figure 2: Geologic map of the Lake Superior iron ore district, Canada and United States of America, showing the Gunflint-Vermillion, Mesabi, Cuyuna, Gogebic, Menominee and Marquette Range banded iron-formations, the type localities of "Superior-type BIF" deposited on the marine shelf of the Archean craton (modified from Marsden 1968).

The Mesabi Range contributed 70-75% of the total ore production. In 1965, direct-shipping ore contained 51-61% iron, and pellets produced from quartz-magnetite BIF 60-65% iron. Manganese-rich iron ore (5.6-14.8% Mn) was mined in the Cuyuna Range, contrasting with the low Mn-content of ore in the rest of the district (mostly < 1% Mn; Marsden 1968). Other publications include those of Goodwin (1956) on the petrography of the Gunflint BIF, Morey and Southwick (1993) on manganese in the Cuyuna Range, Morey and Southwick (1995) on stratigraphic correlation in the Lake Superior district, Morey (1999) on enriched high-grade ore (50-61% Fe) in the Biwabik BIF of the Mesabi Range, Farley and McKeon (2015) on Late Proterozoic-Paleozoic helium ages in botryoidal red hematite from the Gogebic Range, and Losh and Rague (2018) on the hydrothermal oxidation in the Biwabik iron formation by low-T (175°C) fluids expelled from the foreland basin during the 1.85 Ga Penokean Orogeny.

Photograph MichiganHemBIF: Oxide-facies Negaunee BIF, low metamorphic grade, Marquette mining district, Michigan. Folded hematite-quartz banded iron-formation. Dark blue-grey mesobands of specular hematite (0.5-1 mm, non-magnetic) alternate with red mesobands of hematite-stained chert (hard > steel). The marker pen is 10.5 cm long. Display boulder at the entrance of the C.C. Little Building, University of Michigan at Ann Arbor, identical in petrography to the Negaunee Iron Formation shown in the cover photograph of Economic Geology, v. 68, no.7, 1973. The legend by James reads: Jaspilite forming the upper part of the Negaunee Iron Formation of the Marquette district, Michigan, composed of red mesobands of chert stained by dispersed hematite and blue-grey mesobands of specular hematite. The outcrop is at Jasper Knob, Negaunee, Michigan.

5. Proterozoic iron formations in the Quadrilatero Ferrifero, Brazil

In 2017, Brazil was the largest exporter of iron ore in the world before the tailings dam disaster in Minas Gerais forced the temporary closure of mines. Open pits in "itabirite" of the Quadrilatero Ferrifero in the state of Minas Gerais contributed most of the production, a position challenged by iron ore mined in the Serra dos Carajas 500 km south of the Amazon River, now the largest district in South America on a resource basis (Rosière et al. 2018). Resource estimates in 1991 were: 17.9 billion metric tons of ore in the Carajas region (geologic reserves >60% Fe), and 17.1 billion tons in Minas Gerais (geologic reserves; Companhia Vale do Rio Doce) compared to 14.6 billion tons in the Hamersley district of Australia (resources >50% Fe; Machamer et al. 1991).

An overview of the geology of the Proterozoic iron formations (Superior-type) in the Minas Gerais district (see Fig. 3) is given in Rosière et al. (2008). Other publications include those of Klein and Ladeira (2000) on BIF petrology and geochemistry, Ribeiro and Carvalho (2002) on iron enrichment by weathering processes, Spier et al. (2003) on the geology and geochemistry of iron ore in the Aguas Claras and Pico mines, Rosière and Rios (2004) and Dalstra and Rosière (2008) on the origin and structural control of high-grade hematite ores, and Spier et al. (2008) on the mineralogy and trace-element geochemistry of the iron ore.
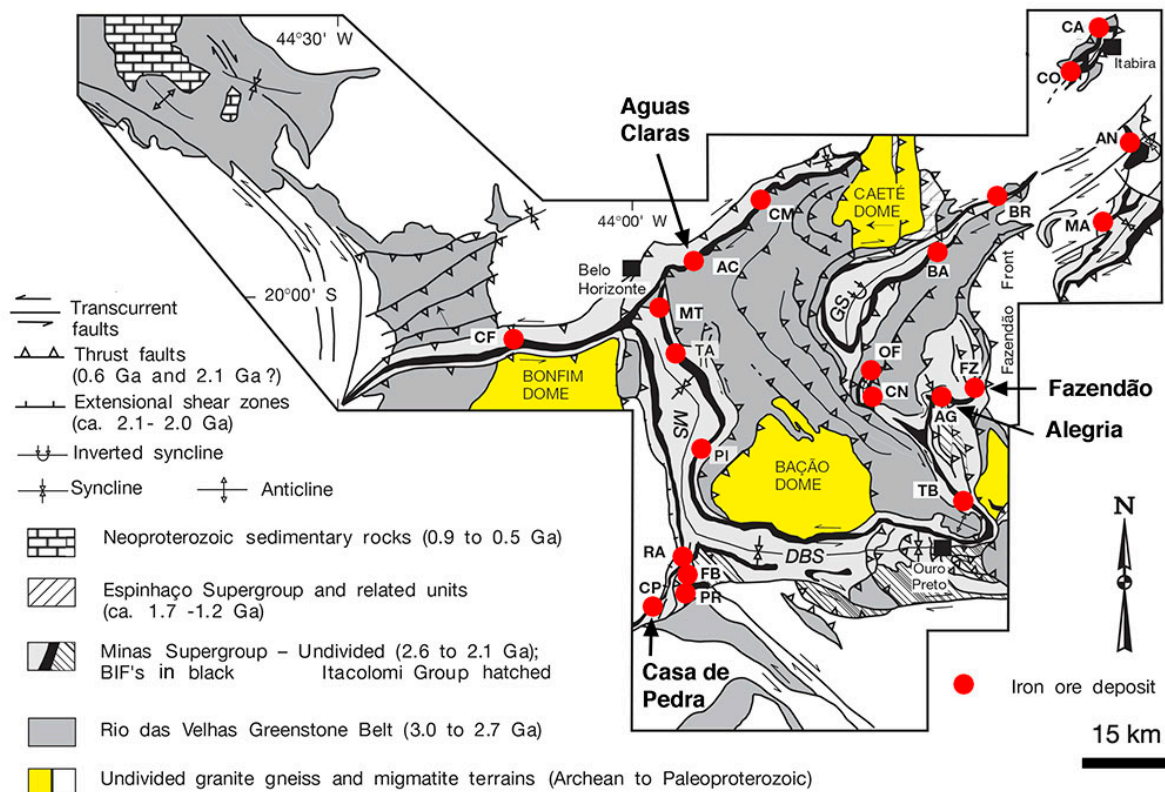
Figure 3: Geologic map of the Quadrilatero Ferrifero iron ore district in Minas Gerais, Brazil, showing the locations of the Alegria, Aguas Claras, Casa de Pedra and Fazendão mines (modified from Rosière and Rios 2004).

Carlos Alberto Rosière contributed all photographs from Minas Gerais.

Photograph MinasG-AlegriaBIF: Alegria mine, eastern Quadrillatero Ferrifero (Fig. 3). Primary ankerite-quartz-hematite/martite banded iron formation with minor amphiboles. The drill core is 5 cm thick.

Photograph MinasG-AguasClaras: Aguas Claras mine, western Quadrillatero Ferrifero (Fig. 3). Coarse-grained remobilized dolomite (Dol) interlayered with fine-grained primary quartz + carbonate + opaque martite/hematite bands. Crossed polarized transmitted light, the scale bar is 800 microns long.

Photographs MinasG-CasaPedra1 and 2: Casa de Pedra mine, southern Quadrillatero Ferrifero (Fig. 3), drill core P16050, A150, R130. Hematite-cemented carbonate dissolution breccia: fragments of dolomite stained by dispersed hematite are cemented by blue-grey specular hematite. The drill core is 5 cm wide.

Photographs MinasG-Fazendão1 and 2: High-grade (68% Fe) hematite ore, Fazendão mine in the eastern Quadrillatero Ferrifero (Fig. 3). Folded and crenulated metamorphic foliation in hematite ore, hematite enrichment by dolomite dissolution took place prior to two deformation events: foliation development followed by crenulation and folding.

6. Proterozoic iron and manganese deposits in South Africa

An overview of Archean and Proterozoic iron formations in South Africa, including those of the Barberton greenstone belt and the Witwatersrand basin is given in Beukes (1973). The Early Proterozoic Superior-type Kuruman iron formation, deposited on platform stromatolitic limestones and dolomites, is described in detail in Klein and Beukes (1989). The Kuruman BIF is about 200 m thick, un-metamorphosed with maximum diagenetic P-T conditions of 110-170°C and < 2 kbar, and consists of meso- and microbanded siderite BIF interbedded with iron shale, stacked cycles of stilpnomelane lutite and microbanded magnetite-siderite ± hematite BIF, and uppermost greenalite-rich BIF. Sedimentary textures such as algal laminae are well preserved, microcrystalline siderite is interpreted as the primary carbonate deposited, and minor subhedral ankerite and Fe-dolomite are interpreted as early to late diagenetic (Klein and Beukes 1989).

The Kuruman iron formation is overlain by a succession of other stable-shelf sedimentary units including, from the oldest to the youngest: the Griquatown iron formation (2432±31 Ma), the Makganyene diamictite above an unconformity marking glaciation, the Ongeluk andesitic lavas, the Hotazel iron formation, and the Mooidraai dolomite (e.g. Bau et al. 1999). The Hotazel Formation of Superior-type dolomite-rich hematite-magnetite-quartz BIF contains three stratigraphic manganese units up to 45 m thick, which constitute the giant Kalahari manganese field (8 billion metric tons at 20-48 wt.% Mn; Tsikos et al. 2003). The primary ore mined (30-39 % Mn; >95% of the total resource) consists of laminated, microcrystalline kutnahorite, braunite and hematite. Constraints on the age of the Mn-rich Hotazel BIF (>2394±26 Ma; Pb-Pb isochron) and on the oxidation state of the Early Proterozoic atmosphere are imposed by the lead and stable isotope systematics of the overlying Mooidraai dolomite (Bau et al. 1999).

Secondary enrichment related to hydrothermal (< 250°C) oxidation and carbonate dissolution produced high-grade (> 42% Mn) black oxide ore replacing the Mn-carbonate and Mn-silicate beds. In the host BIF, the same event produced leached Fe-enriched hematite-quartz BIF, which grades at depth into dolomitized iron formation composed of quartz, partly oxidized magnetite, and CaMn-rich dolomite formed by carbonate re-precipitation (Gutzmer and Beukes 1995; Tsikos et al. 2003). Paleo-magnetic data suggest that the enrichment is linked to the Proterozoic Namaqua orogeny (Evans et al. 2001).

The Kalahari field contains about 50% of the world's land-based manganese resources (Laznicka 1992). A similar Mn-rich BIF occurs in the Urucum district, Mato Grosso do Sul, Brazil (Klein and Ladeira 2004). The Neoproterozoic Urucum succession consists almost entirely of hematite-chert BIF (jaspilite) lacking magnetite, and contains siliceous Mn-horizons composed of braunite, cryptomelane, some pyrolusite and authigenic aegirine. The iron ore resources are estimated at 36 billion metric tons of hematite-rich ore, and 608 million tons of manganese ore (Klein and Ladeira 2004). Other manganese horizons in Superior-type BIF are reviewed in the Economic Geology Special Issue on manganese ore deposits (1992, vol. 87, no. 5).

7. Archean-Proterozoic iron formations, Pilbara, Western Australia

The volcano-sedimentary succession of the Mt Bruce Supergroup in the Pilbara region of Western Australia unconformably overlies the granite-greenstone basement of the

Mesoarchean Pilbara Craton. The basal Fortescue Group (4000 m thick) of flood basalt, tuff, sandstone and shale is conformably overlain by the Hamersley Group (2500 m), which is subdivided into (oldest to youngest): the Marra Mamba BIF (180 m), Wittenoom Dolomite (150 m), Mt Sylvia Formation (30 m), Mt McRae Shale (90 m), Brockman BIF (600 m), Weeli Wolli Formation (450 m), Woongarra Volcanics (730 m), and Boolgeeda BIF (210 m; Trendall and Blockley 1970). Zircons from a tuff bed in the upper Marra Mamba BIF gave a U-Pb age of 2597±5 Ma, zircons from a tuff bed in the upper Wittenoom Dolomite 2561±8 Ma, and zircons from a third tuff bed in the upper Brockman BIF 2470±4 Ma indicating deposition from the Late Archean to the Early Proterozoic (Trendall et al. 1998). The hard resistant iron formations form the Hamersley Range, a topographic high plateau incised by deep canyons (Fig. 4).
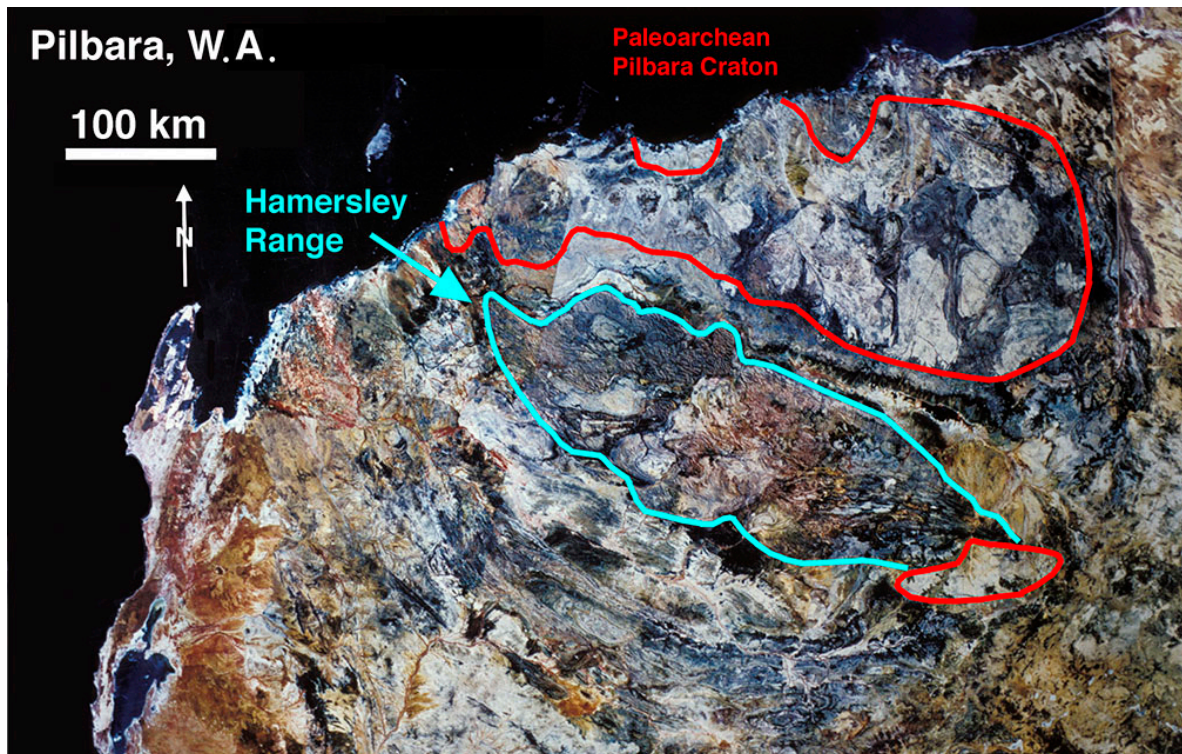
Figure 4: Landsat image from the 1980s of the Pilbara region, Western Australia, showing the approximate outcrop area of the Archean granite-greenstone terrane of the Pilbara Craton (up to 3.5 Ga old), unconformably overlain by the Fortescue Group flood basalt succession, and by the Hamersley Group banded iron-formations (2.6-2.4 Ga) forming the high plateau of the Hamersley Range.

The BIFs (24-34 wt.% Fe) are meso- and microbanded. Marker bands are traceable over 10s of kilometers. They are composed of chert alternating with carbonate, hematite, magnetite, stilpnomelane, riebeckite, apatite and pyrite, in the order of abundance. The carbonates include ankerite, siderite (some Mg-rich), dolomite and calcite. Riebeckite is confined to narrow zones in the iron formations and occurs in two forms: (1) massive mesobands of felted acicular crystals, which pass into lateral equivalents of different mineral composition, and (2) seams of blue asbestos (crocidolite), fibres oriented perpendicular to the walls, which terminate without lateral continuation (Trendall and Blockley 1970). In the Marra Mamba BIF, siderite + dolomite-ankerite and pyrite-pyrrhotite are common in the lowermost part, whereas dolomite-ankerite and calcite predominate in the uppermost part. Minnesotaite and talc are locally present indicating burial metamorphic conditions of the prehnite-pumpellyite facies (100-300°C; Klein and Gole 1981).

The Hamersley succession dips gently south and is essentially un-deformed in the northern half of the range, gently folded in the center, and increasingly deformed into east-striking folds approaching the Proterozoic mobile belts bordering the craton to the south.

The Ophthalmia orogenic cycle at 2.2-2.1 Ga was succeeded by periods of extension, dolerite dyke intrusion, and erosion marked by two unconformities in the stratigraphic succession. The first at ca. 2.05 Ga has a basal conglomerate containing BIF clasts, and the second at ca. 1.95 Ga a conglomerate containing clasts of massive hematite ore (Taylor et al. 2001; Thorne et al. 2014).

The two main mining companies are BHP and Rio Tinto, each exporting about 300 million metric tons of iron ore per annum (2017-2018). The ore reserves and resources reported by Rio Tinto in March 2015 (The West Australian, March 9, 2015, page 41) amounted to: Hamersley Brockman ore: 2.99 billion metric tons at 61.7% Fe; Brockman process ore: 1.14 billion tons at 57.3% Fe; Marra Mamba ore: 1.47 billion tons at 61.6% Fe; Detrital ore: 642 million tons at 61.2% Fe. Brockman ore bodies such as Mt Tom Price (900 Mt) and Mt Whaleback (1400 Mt) consist of massive hematite extending to >400 m depth, and are interpreted as related to oxidation during hydrothermal fluid flow at 2.1-2.0 Ga (Rasmussen et al. 2007), consistent with the presence of eroded hematite clasts in 1.95 Ga conglomerate (Taylor et al. 2001; Thorne et al. 2004, 2009, 2014).

The Marra Mamba and some Brockman ore bodies consist of hematite and goethite extending to about 100 m depth. Primary magnetite is oxidized to hematite (martite), iron silicates and carbonates are oxidized and hydrated to goethite, and other carbonates and quartz are leached or replaced by goethite. These ore bodies are laterally extensive, related to the present land surface, and probably formed during the Cretaceous by supergene enrichment (Taylor et al. 2001).

Photograph HamersleyBIF1: Early Proterozoic (2.5 Ga) Brockman iron formation, mainly chert-iron oxide sedimentary facies, Hamersley Range, Karijini National Park south of Wittenoom, Three Gorges lookout, Pilbara, Western Australia, August 1987.

Photograph HamersleyBIF2: Early Proterozoic (2.5 Ga) Brockman iron formation, low metamorphic grade, Hamersley Range, Karijini National Park, Wittenoom Gorge, Pilbara, Western Australia, August 1987. Mesobanded chert-magnetite iron formation with brecciated internal zones (carbonate dissolution breccia?), the card for scale is 9 cm long.

Photograph HamersleyBIF3: Early Proterozoic (2.5 Ga) Brockman iron formation, Wittenoom Gorge, asbestos mine at the southern end of the gorge. Grab sample of Brockman Iron Formation from the mine dump, Hamersley Range, Pilbara, Western Australia. Mesobanded quartz-magnetite BIF with minor hematite: fine-grained (0.5 mm) magnetite mesobands (1-15 mm) alternate with red-grey hematite-bearing chert mesobands (weakly magnetic to non-magnetic). The chert mesobands are microbanded by 0.1 mm thick laminae of iron oxides. Intercalated are beds of dark grey chert with disseminated magnetite (2-5%), and one bed (2.5 cm thick) of medium-grained yellow tuffaceous (?) siltstone (no reaction 15% HCl). Accessory riebeckite (blue asbestos) forms discontinuous, 1-2 mm thick seams parallel to the mesobands.

Photograph HamersleyBIF4: Brockman banded iron formation, Hamersley Range, Pilbara, Western Australia. BIF composed red hematite-stained chert mesobands, dark grey specular hematite bands (non-magnetic), and discontinuous yellow bands of fibrous silicified riebeckite (Tiger Eye semi-precious stone). The Australian 2 Dollar coin is 20 mm across. Clarke Earth Science Museum, the University of Western Australia.

Photograph HamersleyBIF6: Marra Mamba banded iron formation, Hamersley Range, Pilbara, Western Australia. Weathered chert-hematite banded iron formation with silicified riebeckite bands forming the "tiger eye" semi-precious stone (opalized crocidolite asbestos), locality near Mount Brockman, 55 km northwest of Tom Price town. The Swiss knife is 9 cm long. Display at the Geological Survey of WA Core Library, corner Broadwood and Hunter Street, Kalgoorlie, July 2019.

Photograph HamersleyHematite: Brockman banded iron formation, Hamersley Range, Pilbara, Western Australia. Massive metasomatic hematite ore (>60 wt.% Fe), Mount Tom Price mine. The Australian 2 Dollar coin is 20 mm across. Clarke Earth Science Museum, the University of Western Australia, Perth.

Photograph HamersleyHemGoe: Supergene hematite-goethite ore forming the caprock of the Brockman 2 and 4 hematite ore bodies (>60% Fe), Hamersley Province, Pilbara Craton, Western Australia. Rio Tinto transferred ore grading about 55% Fe to the "low-grade" stockpiles not sold at the time of the mine visit in 2012. The matchstick is 42 mm long.

Photograph HamersleyGoethite: Brockman banded iron formation, Hamersley Range, Pilbara, Western Australia. Massive supergene goethite ore (>60 wt.% Fe), probably formed by the replacement of primary iron carbonate or silicate, Mount Tom Price mine. The Australian 2 Dollar coin is 20 mm across. Clarke Earth Science Museum, the University of Western Australia, Perth.

8. Miocene fluviatile ironstones, Robe River, Pilbara, Western Australia

The Miocene fluviatile channel iron ore deposits in the Pilbara have few counterparts in the world, and are unique in size (>7 billion tons; Morris and Ramanaidou 2007). Ore reserves and resources reported by the Rio Tinto iron ore division in March 2015 (The West Australian, March 9, 2015, page 41) amounted to 3.4 billion tons at 57% Fe. The channel deposits were discovered in the Robe River valley, where they formed prominent mesas rising 50 m above the plains (Fig. 5). The Robe and Fortescue river plains topographically separate the Archean Pilbara craton in the north from the Hamersley Range in the south (Fig 4). Mining of the iron ore capping the mesas began in 1972 when Robe River Iron Associates, a subsidiary of Cleveland Cliffs Iron Company in Michigan, shipped the first processed ore to Cape Lambert for export. In 1994/95, production had increased to 25 million tons per year (Robe River Communications and Public Relations, December 1995: Reflections – Robe's 20 years). The company was taken over by Rio Tinto about 10 years later.

Figure 5: Historic pre-mining photograph of the ironstone-capped mesas in the Robe river valley forming the foothills of the Hamersley Range, Pilbara region, Western Australia. Robe River Associates, Communications and Public Relations prospectus, December 1995: Reflections – Robe's 20 years.

The iron ore is 4-50 m thick (average: 30 m), and consists of goethite and subordinate hematite forming detrital granules, ooliths, pisoids, and ferruginized wood fragments cemented by goethite and lesser, variably oxidized siderite. Three types of mesa iron ore are distinguished: (1) a bedded facies with claystone lenses, (2) a massive hard facies of closely packed ooliths and wood fragments with zones of reworking, and (3) a conchoidal hard facies with silica cement related to silcrete-calcrete formation. The ore mined in 1995 averaged 57.1% Fe (Table 1). Sintering (calcination) increased the average iron content to 63% by driving off the volatiles. Sinter fines were the main export product in 1995 apart from minor pellet and lump iron ore (Robe River Communications and Public Relations).

The Robe River iron ore was deposited in meandering river channels, which reached widths of more than 1 km during periods of flooding perhaps related to high seawater levels in the Indian Ocean. The ferric iron was derived from deeply weathered flood basalts of the Archean Fortescue Group, and from banded iron formations in the Hamersley Range (Morris and Ramanaidou 2007). Subsequent uplift and erosion by the present river system lead to the formation of mesas capped by the resistant ironstone. Most of the Pilbara channel iron ore deposits are Miocene in age but some are Eocene-Oligocene or Pliocene (MacPhail and Stone 2004; Morris and Ramanaidou 2007; Haest et al. 2012).

Photograph RobeIronstone95a: Miocene fluviatile ironstone capping a mesa near the town of Pannawonica in the Pilbara, Western Australia, note the Robe river below and the 350 car iron-ore train in the background. Photograph scanned from: Robe River Iron Associates, Communications and Public Relations prospectus, December 1995.

Photograph RobeIronstone95b: Aerial photograph of the Mesa J iron ore mine in Miocene fluviatile ironstone, note the green Robe river valley, July 1995, Pilbara, Western Australia. Photograph scanned from: Robe River Iron Associates, Communications and Public Relations prospectus, December 1995.

Photograph RobeIronstone95c: Iron ore products of Robe River Iron Associates in 1995: pellets (top left, hematite), lump ore (top right, goethite) and sinter fines (mixed goethite-hematite, bottom). The main product was sinter fines upgrading the primary Miocene ironstone to 63% Fe. Photograph scanned from: Robe River Iron Associates, Communications and Public Relations prospectus, December 1995.

Photograph RobeIronstone1: Robe River Miocene fluviatile ironstone, Pilbara, Western Australia. Detrital to oolitic, limonite-bearing goethite ironstone, 20 cm thick core drilled for grade control into the mesas of the Robe river valley. Clarke Earth Science Museum, the University of Western Australia, Perth.

Photograph RobeIronstone2: Miocene fluviatile ironstone, Pilbara, Western Australia. Oolitic hematite-bearing goethite ironstone, unknown location, probably from a mesa in the Robe river valley, the Australian 2 Dollar coin is 20 mm across. Clarke Earth Science Museum, the University of Western Australia, Perth.

Table 1:	Average composition of iron ore from fluviatile (Robe River) and marine						
	ironstone deposits in Australia, the United States, and Europe.						
Country	Australia	USA	England	France	France	Germany	Germany
Deposit	Robe River	Clinton	Cleveland	Lorraine	Lorraine	Peine	Peine
Type	oolitic +	oolitic +	oolitic	oolitic	oolitic	detrital	detrital
(Bed)	detrital	detrital		Red Bed	Grey Bed	Buelten	Lengede
Year	1995	1933	1933	1914	1914	1914	1914
Fe (wt.%)	57.10	37.00	29.93	42.39	31.82	32.90	34.40
FeO			36.91				
Fe2O3	> FeO	> FeO	1.77	>FeO	>FeO	>FeO	>FeO
SiO2	5.70	7.14	8.51	9.90	7.90	4.40	7.80
Al2O3	2.64	3.81	6.12	5.50	2.30	0.80	3.70
TiO2	0.21		0.36				
MgO	0.06		3.75	0.50	0.50	0.60	0.08
CaO	0.40	19.20	5.54	6.20	19.00	17.00	14.60
Na2O	0.02		0.05				
K2O	0.01		0.03				
CO2			20.70	4.90	14.30		
H2O	9.40		14.05	10.10	8.00		
L.O.I.			34.75	15.00	22.30	20.00	17.00
Mn	0.10	0.23	0.33	0.25	0.30	4.50	0.80
P	0.04	0.30	0.57	0.79	0.74	1.10	1.60
S	0.03	0.08	0.05	0.04	0.04		
V	0.01		0.05	0.20	0.20		
As	< 0.01		0.02				
Data sources: Beyschlag et al. (1914), Lindgren (1933), Walter (1995), Robe River							
Associates, Communications and Public Relations, December 1995. Trace elements							
in Robe River ore: Bi, Co, Cr, Cu, Mo, Ni, Sn = 20-50 ppm, Zn 100 ppm.							

## 9. Mesozoic marine oolitic and detrital ironstones in Europe

In Europe, marine shelf ironstones located in the vicinity of equally large deposits of coking coal provided most of the raw material for the increase in steel production during the industrial revolution in the 19th and early 20th century. After about 1860, iron from other local sources such as bog iron ore, "black band" siderite mined together with coal, and siderite veins and replacement deposits became either insignificant or progressively subordinate. The invention of the Thomas basic process in 1878 allowed the removal of phosphorus as slag, and enabled the smelting of low-grade, apatite-bearing oolitic ironstones to pig iron for steelmaking (e.g. Beyschlag et al. 1914). The slag could be sold as a product for agricultural fertilizer. Noteworthy in terms of past production are the Lorraine "minette" district in France and Luxembourg (3 billion metric tons at 30% Fe, 1860-1987; Walter 1995), the Cleveland-Northampton district in England (1.76 billion tons at 29% Fe, 1846-1975; Dunham et al. 1978), and the Peine-Salzgitter district in northern Germany (308 million tons at 28% Fe, 1880-1982; Walter 1995). The average composition of the iron ores mined is listed in Table 1.
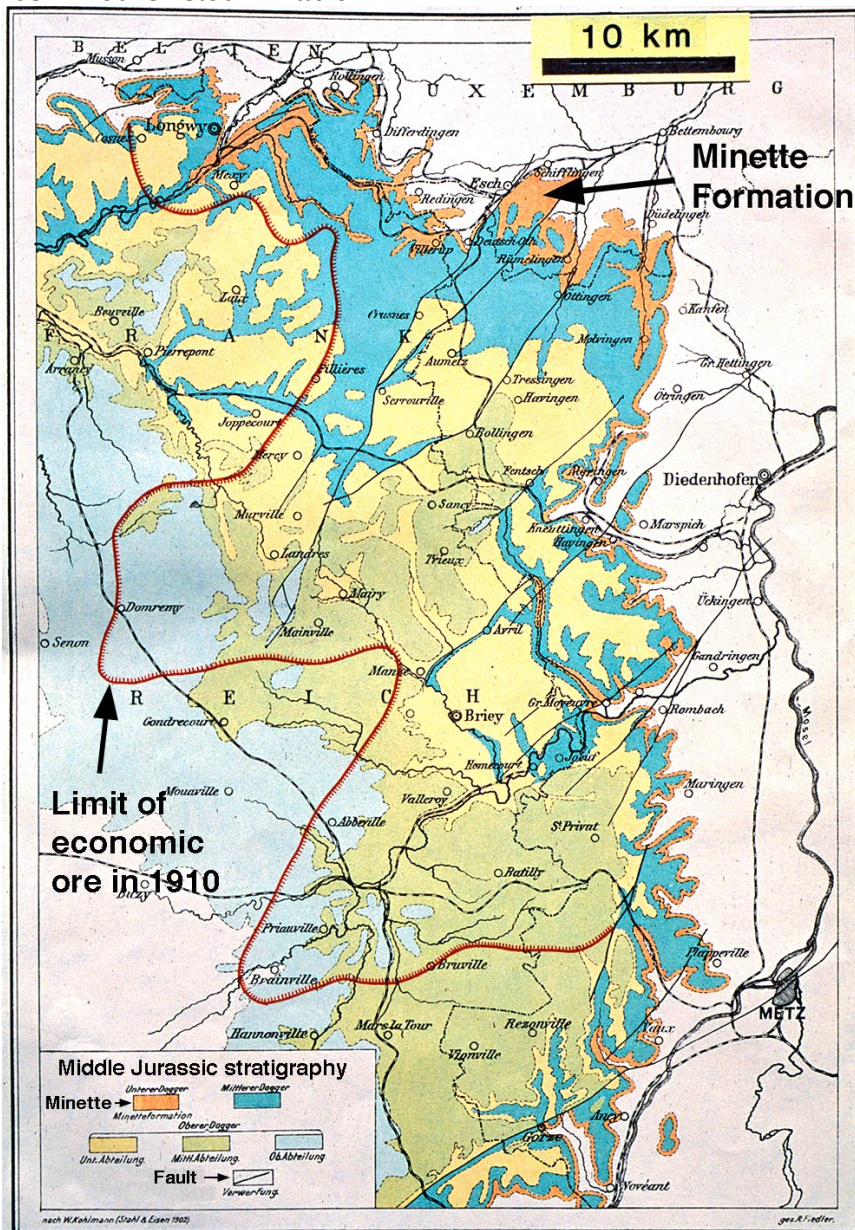
Figure 6: Geologic map 1:200,000 of the Lorraine mining district in France and Luxembourg modified from the iron ore section of the 11th International Geologic Congress 1910. The Middle Jurassic oolitic iron ores crop out along the eastern margin of the Paris sedimentary basin and dip west at 3° on average.

Most Mesozoic and Paleozoic oolitic ironstones are chamosite-type in the classification of Mücke and Farshad (2005) and Mücke (2006). The primary ore consisted mainly of Fe-chlorite and siderite, variably oxidized and enriched by early diagenetic processes prior to the formation of very low metamorphic grade goethite, hematite and magnetite. Both publications also contain up-to-date references, transmitted and reflected light photographs of ooliths, whole-rock major and trace element analyses, and electron microprobe analyses of primary Fe-chlorite (chamosite, thuringite) and siderite from the deposits reviewed below.

France: The Middle Jurassic (Aalenian) ironstones of the giant Lorraine district are part of the marlstone-limestone platform succession, which crops out along the eastern margin of the Paris sedimentary basin (Fig. 6), bounded to the north, northeast and east by exposed Paleozoic basement of the Ardennes, Eifel and Vosges mountains, all part of the Variscan orogenic belt. The ore-bearing formation is capped by shale and marlstone 20-30 m thick, dips west at 3° on average, and increases in thickness from 15-20 m in the outcrop area to 60 m going west (Fig. 7). The ironstones are subdivided into an upper calcareous and a lower siliceous group. The Red Bed (typical thickness: 2.9 m), Upper Yellow Bed (1.2 m), Lower Yellow Bed (1.5 m), and Grey Bed (3.7 m) form the calcareous group, and the Brown Bed (2.4 m) and Black-Green Bed (2.6 m) the siliceous group. The ironstone beds are separated by intercalated marlstones up to 5 m thick and are also underlain by marlstone. The thickness of an individual ore bed varies due to intercalated limestone lenses and marlstone partings up to a maximum 7 meters. The most persistent is the Grey Bed with an average of 3-4 m and contents of 28-40 wt.% Fe, 10-15% CaO and 5-10% SiO_2 (Table 1). The iron content is confined to ooliths averaging 0.25 mm in diameter, which lack detrital cores and consist mainly of red-brown goethite, lesser green Fe-chlorite, and minor siderite. Magnetite occurs locally in the Longwy-Briey sub-basin of the deposit, whereas pyrite is rare. Within an ore bed, there is an increase in grain size and a change green to brown (Fe^{2+} to Fe^{3+}) from bottom to top. Modern track-less mining of the ore beds was by room-and-pillar with progressive pillar removal to recover up to 95% of the ore in place prior to caving of the hanging wall. The ironstones are displaced up to 150 m at NE-striking normal faults (Fig. 7), which are widely spaced and had little effect on mining except for breaching the hanging wall marlstone seal causing the influx of groundwater. Total ore production from the district was 38 million metric tons (Mt) in 1910, 49 Mt in 1930, 63 Mt in 1960, and 11 Mt in 1987 until mine closure in 1993. The remaining reserves are estimated at 6-7 billion metric tons (Beyschlag et al. 1914; Lindgren 1933; Parisot and Schmit 1994; Walter 1995).
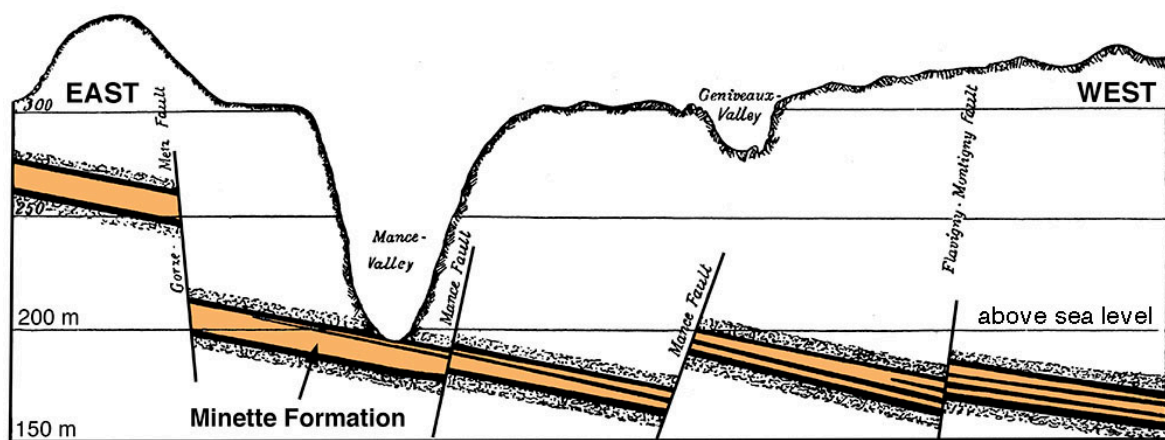
Figure 7: Schematic cross section through the ironstone beds (black) of the Jurassic Minette Formation dipping west into the Paris sedimentary basin (modified from Beyschlag et al. 1914). The vertical scale is ten times the horizontal one.

England: The ironstones of the Cleveland Hills, Frodingham and Northampton districts in Yorkshire and Lincolnshire, England, occur in Lower to Middle Jurassic shale-sandstone successions, which outcrop along the northwestern margin of the London sedimentary basin and dip at shallow angles southeast. The thickness of the ironstone beds mined varied from 2-4 m. In the Cleveland Hills district, the most productive of the three, mining took place in the Main (1.8-3.5 m) and Pecten (0.6-1.4 m) oolitic beds, both locally extracted together where the intercalated shale (1 m) thinned (Beyschlag et al. 1914). Chamosite ooliths are set in a matrix of fine-grained chamosite and siderite, the siderite in part recrystallized to subhedral rhombs (FeO/Fe$_2$O$_3$ ratio = 21:1; Table 1). Chamosite (34 vol.%) and siderite (35%) both contribute to the average 29-30 wt.% Fe in the ore. The Main ironstone contains accessory barite, pyrite, sphalerite and galena, the latter commonly replacing shells, and is intercalated with a thin upper "oolitic" bed of pyrite (0.11 wt.% Ni + Co, 0.15% PbO, 0.015% CuO; Lindgren 1933).

Germany: The Peine-Salzgitter iron ore district is centered on the cities of Peine and Braunschweig in the state of Lower Saxony, north Germany. Oolitic and detrital ironstones occur in the Jurassic-Cretaceous shelf succession north of the Harz and northwest of the Flechtingen basement uplifts. Far-field stress during the Cretaceous, early phases of the Alpine orogenic cycle, initiated the uplift of the Variscan basement blocks at WNW-striking faults, and accelerated the movement of the Permian Zechstein salt into pillows and stocks, which dome or pierce the Mesozoic platform cover (Fig. 8).
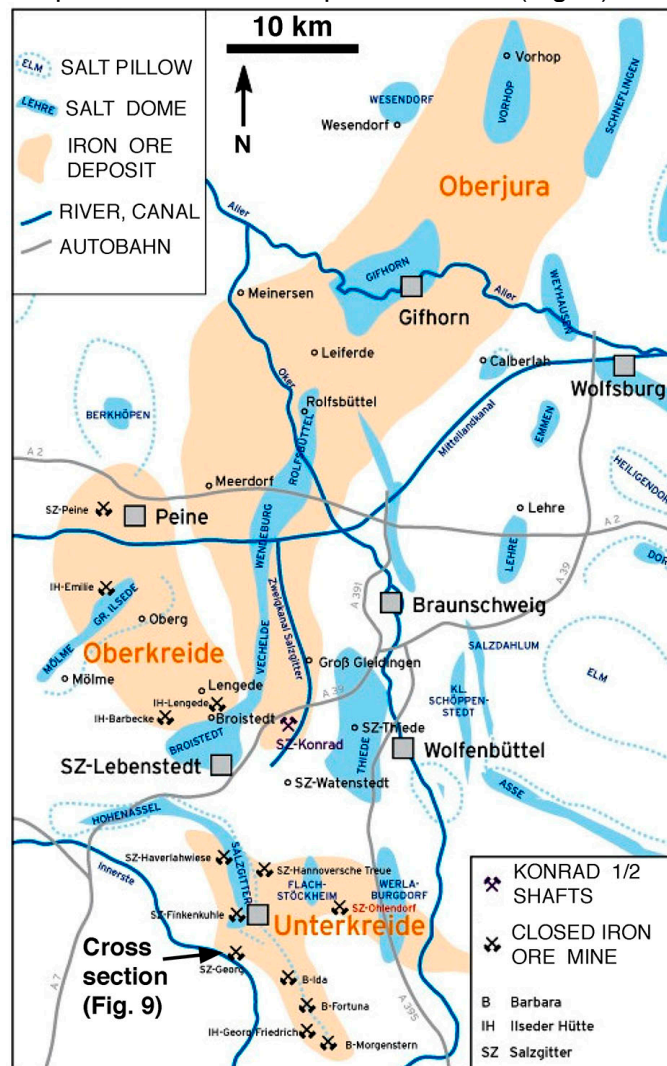
Figure 8: Simplified geologic map of the Peine-Salzgitter iron ore district, Lower Saxony, north Germany, illustrating the areal extent of Upper Jurassic (Oberjura), Lower Cretaceous (Unterkreide) and Upper Cretaceous (Oberkreide) ironstone deposits (modified from Kolbe 1957).

The Upper Jurassic (Oxfordian) iron ore deposit in the Gifhorn Trough adjacent to a line of salt domes (Fig. 8) contains 1.4 billion metric tons of oolitic goethite ironstone 12-18 m thick. The blind deposit was discovered in 1933 at 660 m depth, and accessed via two shafts (Konrad 1 and 2) sunk from 1957 to 1963. In total, 6.7 million tons of iron ore were mined until 1976, when the mine closed due to non-profitability. The deposit is enclosed in thick shale-marlstone beds providing an effective groundwater seal, and is currently developed as a repository for low to intermediate level radioactive waste (www.bge.de).

Most of the past production from the district has been from Lower Cretaceous (Hauterive, Barrême) siliceous ironstone deposits (production: 165 Mt at 30% Fe) at the margin of the Salzgitter anticlinal salt structure (Fig. 8). These ironstones filled syn-sedimentary graben and half-graben traps, which subsided during the movement of salt into the anticline, a "halokinetic" structural setting perhaps induced by fault reactivation in the basement (Kolbe 1962). At the main fault bounding the half-graben, iron ore more than 100 m thick accumulated (Fig. 9), mainly as goethite ooliths in the Hauterive and predominantly as goethite detritus in the Barrême. Re-sedimented Jurassic fossils indicate that the detritus was derived from oxidized siderite nodules eroded from paleohighs by the shallow Cretaceous sea. Ironstone sedimentation ceased in the Albian, when erosion worked its way down into the underlying Triassic sandstones and the thick Hils sandstone covered the deposits (Kolbe 1962). Continuing salt movement during the Cenozoic tilted many deposits into a steeply dipping or sub-vertical position (Fig. 9).
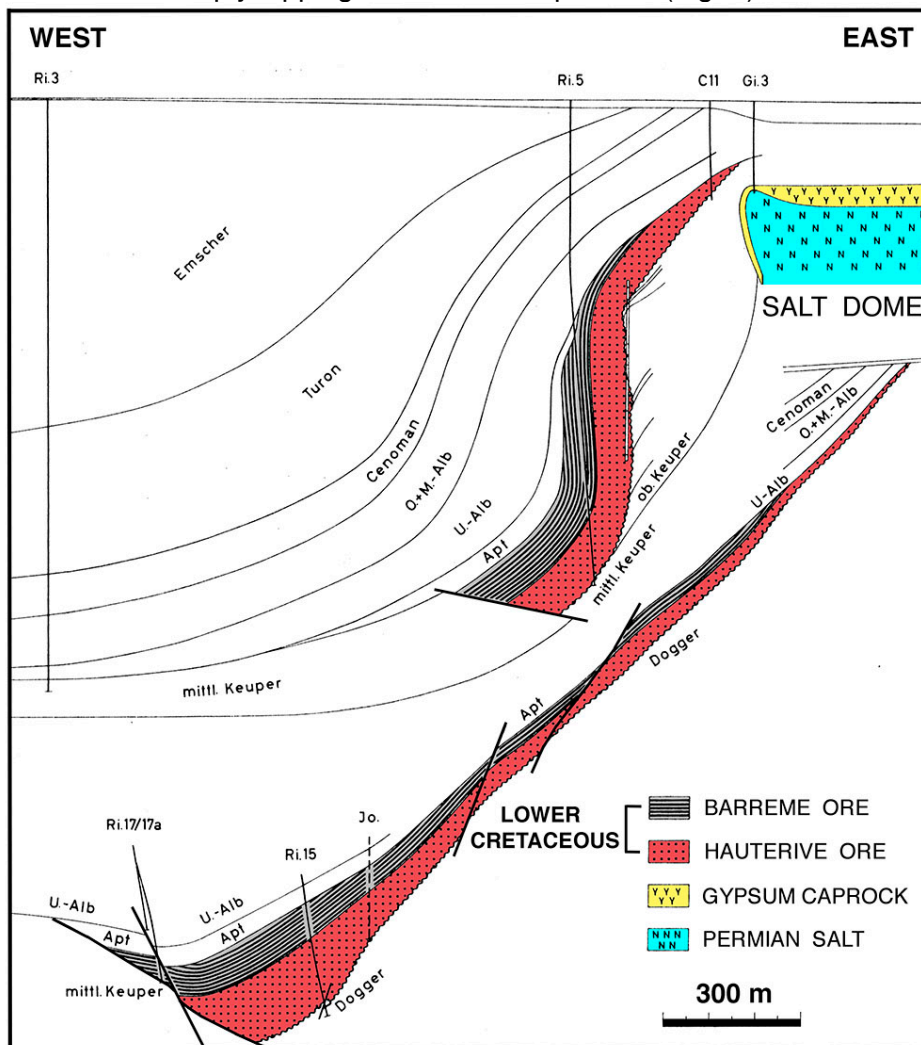
Figure 9: Two west-east cross sections through the ironstone deposit in the halokinetic Ringelheim half-graben at the margin of the Salzgitter salt dome (modified from Kolbe 1962).

The remaining production in the Salzgitter district (143 Mt at 25% Fe; Walter 1995) came from Upper Cretaceous (Santonian) detrital ironstones deposited as transgression conglomerates in littoral marine basins. They consist of goethite crusts and fragments cemented by calcareous clay and/or ferroan calcite. Siderite nodules in exposed Albian shales were eroded, oxidized, reworked, fragmented, and then concentrated as lag deposits on the shelf in near-shore depressions. The ironstone bed mined was 5-20 m thick, and outcropped in two shallow closed synclines (3-18° dip) at the villages of Lengede and Bülten-Adenstedt near the town of Peine (Fig. 8). The iron content of the ore varied from 28-35 wt.% Fe, the manganese from 0.8-4.5% Mn, and the phosphorus from 1.1-1.6% P (Table 1). The calcareous ore was ideally suited for the Thomas basic process, and needed no or little admixed siliceous ore from the nearby Salzgitter mines for fluxing. The ore reserves in 1913 were estimated at 218 million tons (Beyschlag et al. 1914).

Photograph JurassicFeOre1: Upper Jurassic (Oxfordian) oolitic goethite ironstone (Korallenoolith), lower orebody (Unteres Lager) of the Gifhorn Trough deposit. Shaft Konrad 1 at 1180 m depth, Salzgitter-Bleckenstedt, Lower Saxony, Germany. The matchstick is 4 cm long. Ore deposit collection of the Technical University of Clausthal in Clausthal-Zellerfeld.

Photograph JurassicFeOre2: Lower Jurassic (Lias Alpha 3) oolitic goethite ironstone, goethite cast of the ammonite Coroniceras (note the remnant white shell), Friederike mine near Bad Harzburg, northern margin of the Harz basement block, Lower Saxony, Germany. The open Swiss knife is 16 cm tall, collection of the Technical University of Clausthal in Clausthal-Zellerfeld.

Photograph JurassicFeOre3: Lower Jurassic (Lias Gamma) oolitic ironstone, the primary chamosite-siderite oolitic ore (green) is partly oxidized to brown goethite, ironstone bed in the Jurassic-Cretaceous Sack-Hils syncline. The German Pfennig is 16 mm across. Echte mine, Kahlberg north of the villages of Kalefeld and Echte, near Northeim and Einbeck, Lower Saxony, Germany. Ore deposit collection of the Technical University of Clausthal in Clausthal-Zellerfeld.

Photograph JurassicFeOre4: Lower Jurassic oxidized goethite oolitic ironstone (40% Fe) containing minor yellow-brown limonite clasts, ironstone bed in the Jurassic-Cretaceous Sack-Hils syncline. The German 5 Pfennig coin is 19 mm across. Echte mine, Kahlberg north of the villages of Kalefeld and Echte, near Northeim and Einbeck, Lower Saxony, Germany. Ore deposit collection of the Technical University of Clausthal in Clausthal-Zellerfeld.

Photograph CretaceousFeOre1: Lower Cretaceous (Hauterive-Barrême) goethite ironstone composed of ooliths and minor detrital fragments, Red Orebody (Rotes Lager), Haverlahwiese mine, Salzgitter-Bad, Lower Saxony, Germany. The matchstick is 4 cm long. Ore deposit collection Technical University of Clausthal in Clausthal-Zellerfeld.

Photographs CretaceousFeOre2 and 3: Upper Cretaceous (Santonian) detrital ironstone composed of broken goethite crusts and smaller bean-sized fragments, both concentrically banded by dark brown goethite and light brown limonite. White or brown calcite and rare black bitumen partly fill small cavities. The matrix consists of pale brown, sparry (1-2 mm) ferroan calcite (strong reaction 3% HCl), and of 10-15% white-grey calcite shell and coral fragments. Bülten-Adenstedt mine near Peine, Lower Saxony, Germany, "Trümmererz" collected by the author in 1976. The Australian 5 cent coin is 19 mm across.

10. Paleozoic marine oolitic ironstones in North America and Europe

In North America, ironstones occur in the Paleozoic Appalachian fold belt. The Ordovician Wabana ironstones on Newfoundland, Canada, form beds 3-9 m thick in a marine sandstone-shale succession. They were mined in a synform of shallow dip from outcrops at Conception Bay to several kilometers under the Atlantic Ocean. The ore-in-place is estimated at about 2 billion metric tons (Hayes 1931). The brown and green ooliths constituting the fine-grained ore consist of hematite (50-70 vol.%), chamosite (15-25%) and quartz (1-10%) cemented by siderite (0-50%) and lesser calcite (0-1%). Borings

of algae in ooliths suggest the photosynthesis triggered the oxidation of chamosite to goethite-hematite prior to burial (Lindgren 1933).

The Silurian Clinton ironstones extend from New York State south into Alabama, where three beds 2-6 m thick were mined in the Birmingham district. The beds occur in a ferruginous sandstone-shale succession, which overlies Cambro-Ordovician platform limestone and dolomite. The ore consists of hematite-cemented conglomeratic sandstone, hematite ooliths cemented by calcite, hematite concretions, and fossil fragments cemented and replaced by hematite. Primary "hard ore" averaged 37% Fe and 19% CaO (Table 1). Secondary enrichment of the east-dipping ironstone beds to a depth of 60 m upgraded the "soft ore" to about 50% Fe due to calcite leaching (Lindgren 1933). The Birmingham district produced 300 million tons of ore from 1864 to 1967, and retained resources of about 2 billion tons in 1968, when higher grade imported ore led to a sharp reduction in output (Simpson and Gray 1968), and to the subsequent closure of the mines.

In Europe, folded Ordovician ironstones were mined in the Barandian synform near Prague, Czech Republic, and near Schmiedefeld in Thuringia, Germany. Both sedimentary successions are part of the Paleozoic Variscan orogenic belt. The Barrandian one in the central part of the Bohemian Massif comprises shelf quartzite, deeper water shale, spilitized submarine basalt, and two ironstone marker horizons, one in the Llanvirn (Klabava-Osek ore), and the second in the Caradoc (Nucice-Chrustenice ore). The Nucice ironstone bed at the northern limb of the synform is up to 22 m thick, dips 50-60° south, and has been traced over a strike length of 40 km. The primary ore (average 35 wt.% Fe) is dark green to blue-grey, and consists of chamosite ooliths in a schistose siderite matrix. The iron content increased to 44 % Fe after roasting (Beyschlag et al. 1914). Annual ore production in 1914 was 700,000 metric tons. Mining ceased in 1967 after a cumulative production of about 100 million tons (35 Mt Fe). The remaining resource is estimated at 600 million tons (Walter 1995). The ironstone deposits in Thuringia occur in the folded quartzite-shale succession of the Gräfenthal Formation (Arenig to Caradoc). The main ore bed is 15-20 m thick, and consists of chamosite-thuringite ooliths in a siderite matrix (22 wt.% CO_2 on average). The total ore resource was about 100 million metric tons (Beyschlag et al. 1914). Mining ceased in 1971 (Walter 1995).

11. Mesozoic-Cenozoic marine oolitic manganese deposits

The manganese content of ironstones (up to 4.5 % Mn at Peine, Germany) was treated as a bonus prior to 1980 because manganese is a key alloy in steel. Most of the high-grade iron ores processed today contain little manganese, which has to be added to the blast furnace from other sources. Marine oolitic manganese deposits are one such source. In Australia, a large Lower Cretaceous deposit is mined on Groote Eylandt in the Gulf of Carpentaria at the north coast. The oolitic bed of black Mn-oxides (mainly cryptomelane and pyrolusite) averages 3-4 m in thickness and is part of a sandstone-shale-marlstone succession up to 100 m thick deposited un-conformably on Precambrian quartzitic sandstone. The bedding dips at shallow angles west. The pre-mining ore reserves (37-53 wt.% Mn) were estimated at 190 million metric tons, and the potential resources at 300 Mt (McIntosh et al. 1975). Lateritic weathering caused the re-distribution and enrichment of Mn-oxides in the upper part of the ore body (Pracejus and Bolton 1992).

Even larger deposits of pyrolusite and Mn-carbonate in oolitic beds up to 3 m thick occur in Oligocene sandstone-shale-marlstone successions at the periphery of the Black Sea: Nikopol in Ukraine (940 Mt), Chiatura in Georgia (600 Mt), and Bol'shoi Tokmak in Ukraine (490 Mt). The primary ore has contents of 20-25 % Mn, and enriched oxide ore averages 40-50 % Mn and 0.16 % P (Lindgren 1933; Varentsov 1964; Varentsov and Rakhmanov 1974; Laznicka 1992). Ore deposition is interpreted as related to the upwelling of seawater rich in dissolved Mn^{2+} from the deep euxinic part of the Black Sea basin followed by precipitation on the marine shelf. Conditions in the restricted basin were probably similar to those recorded in the Baltic Sea (Huckriede and Meischner 1996).

12. References

Angerer T, Hagemann SG (2010) The BIF-hosted high-grade iron ore deposits in the Archean Koolyanobbing greenstone belt, Western Australia: Structural control on synorogenic- and weathering-related magnetite-, hematite- and goethite-rich iron ore. Econ Geol 105: 917-945

Angerer T, Hagemann SG, Danyushevsky LV (2012) Geochemical evolution of the banded iron formation-hosted high-grade iron ore system in the Koolyanobbing greenstone belt, Western Australia. Econ Geol 107: 599-644

Bau M, Romer RL, Lueders V, Beukes NJ (1999) Pb, O and C isotopes in silicified Mooidraai dolomite (Transvaal Supergroup, South Africa): implications for the composition of Paleoproterozoic seawater and 'dating' the increase of oxygen in the Precambrian atmosphere. Earth Planet Sci Letters 174: 43-57

BGR, Bundesanstalt fuer Geowissenschaften und Rohstoffe (1977, 1978): The iron ore deposits of Europe and adjacent areas (explanatory notes to the international map of the iron ore deposits of Europe 1:2,500,000). Volume 1 (1977): Text and figures, 418 pp. Volume 2 (1978): Lists and tables, 386 pp. BGR Schriften, Hannover.

Beukes NJ (1973) Precambrian iron-formations of southern Africa. Econ Geol 68: 960-1004

Beyschlag F, Vogt JHL, Krusch P (1914) The deposits of the useful minerals and rocks, their origin, form and content (translated by S J Truscott). MacMillan, London, 1262 pp.

Czaja AD, Johnson CM, Beard BL, Roden EE, Weiqiang L, Moorbath S (2013) Biological Fe oxidation controlled deposition of banded iron formation in the ca. 3770 Ma Isua supracrustal belt (West Greenland). Earth Planet Sci Letters 363: 192-203

Dalstra HJ, Rosière CA (2008) Structural controls on high-grade iron ores hosted by banded iron formation: a global perspective. Reviews in Economic Geology, v. 15, pp. 73-106

Douglas RJW (1970) Geology and economic minerals of Canada. Geological Survey of Canada, Economic Geology Report no. 1, 838 pp

Dunham K, Beer KE, Ellis RA, Gallagher MJ, Nutt MJC, Webb BC (1978) United Kingdom. In: Bowie SHU, Kvalheim A, Haslam HW (eds) Mineral deposits of Europe, Volume 1: Northwest Europe, pp. 263-317. Inst Min Metall London.

Duuring P, Hagemann S (2013) Leaching of silica bands and concentration of magnetite in Archean BIF by hypogene fluids: Beebyn Fe ore deposit, Yilgarn Craton, Western Australia. Miner Deposita 48: 341-370

Evans DAD, Gutzmer J, Beukes NJ, Kirschvink JL (2001) Paleomagnetic constraints on ages of mineralization in the Kalahari Manganese Field, South Africa. Econ Geol 96: 621-631

Farley KA, McKeon R (2015) Radiometric dating and temperature history of banded iron formation-associated hematite, Gogebic Iron Range, Michigan, USA. Geology 43: 1083-1086

Floran RJ, Papike JJ (1978) Mineralogy and petrology of the Gunflint iron formation, Minnesota-Ontario: Correlation of compositional and assemblage variations at low to moderate grades. J Petrol 19: 215-288

Gole MJ (1980) Mineralogy and petrology of very-low-metamorphic grade Archaean banded iron-formations, Weld Range, Western Australia. Am Mineralogist 65: 8-25

Gole MJ (1981) Archean banded iron-formations, Yilgarn Block, Western Australia. Econ Geol 76: 1954-1974

Gole MJ, Klein C (1981) High-grade metamorphic Archean banded iron formations, Western Australia: assemblages with coexisting pyroxenes ± fayalite. Am Mineralogist 66: 87-99

Goodwin AM (1956) Facies relations in the Gunflint iron formation. Econ Geol 51: 565-595

Goodwin AM (1964) Geochemical studies at the Helen iron range. Econ Geol 59: 684-718

Griffin AC (1981) Structure and iron-ore deposition in the Archaean Koolyanobbing greenstone belt, Western Australia. Geol Soc Australia Special Pub no. 7, pp. 429-438

Gross GA (1980) A classification of iron formations based on depositional environments. Can Mineralogist 18: 215-222

Gutzmer J, Beukes NJ (1995) Fault controlled metasomatic alteration of Early Proterozoic sedimentary manganese ores in the Kalahari Manganese Field, South Africa. Econ Geol 90: 823-844

Haest M, Cudahy T, Laukamp C, Gregory S (2012) Quantitative mineralogy from infrared spectroscopic data. II. Three-dimensional mineralogical characterization of the Rocklea channel iron deposit, Western Australia. Econ Geol 107: 229-249

Hayes AO (1931) Structural geology of the Conception Bay region and of the Wabana iron ore deposit of Newfoundland. Econ Geol 26: 44-64

Hofmann HJ, Sage RP, Berdusco EN (1991) Archean stromatolites in Michipicoten Group siderite ore at Wawa, Ontario. Econ Geol 86: 1023-1030

Holland HD (2005) Sedimentary mineral deposits and the evolution of Earth's near-surface environments. Econ Geol 100: 1489-1509

Huckriede H, Meischner D (1996) Origin and environment of manganese-rich sediments within black-shale basins. Geochim Cosmochim Acta 60: 1399-1413

James HL (1954) Sedimentary facies of iron-formation. Econ Geol 49: 235-293

Klein C (2005) Some Precambrian banded iron-formations (BIFs) from around the world: Their age, geologic setting, mineralogy, metamorphism, geochemistry, and origin. Am Mineralogist 90: 1473-1499

Klein C, Gole MJ (1981) Mineralogy and petrology of parts of the Marra Mamba iron formation, Hamersley basin, Western Australia. Am Mineralogist 66: 507-525

Klein C, Beukes NJ (1989) Geochemistry and sedimentology of a facies transition from limestone to iron-formation deposition in the Early Proterozoic Transvaal Supergroup, South Africa. Econ Geol 84: 1733-1774

Klein C, Ladeira EA (2000) Geochemistry and petrology of some Proterozoic banded iron-formations of the Quadrilatero Ferrifero, Minas Gerais, Brazil. Econ Geol 95: 405-428

Klein C, Ladeira EA (2004) Geochemistry and mineralogy of Neoproterozoic banded iron-formations and some selected, siliceous manganese formations from the Urucum district, Mato Grosso do Sul, Brazil. Econ Geol 99: 1233-1244

Kolbe H (1957) Niedersachsens Bodenschätze, Eisenerze. Geogr Rundschau 9: 175-181

Kolbe H (1962) Die Eisenerzkolke im Neokom-Eisenerzgebiet Salzgitter. Mitteilungen aus dem Geologischen Staatsinstitut in Hamburg, Heft 31, pp. 276-308

Krupp R, Oberthür T, Hirdes W (1994) The Early Precambrian atmosphere and hydrosphere: Thermodynamic constraints from mineral deposits. Econ Geol 89: 1581-1598

Laznicka P (1992) Manganese deposits in the global lithogenetic system: Quantitative approach. Ore Geol Rev 7: 279-356

Lindgren W (1933) Mineral deposits, 4th edition. McGraw-Hill, New York, 930 pp.

Losh S, Rague R (2018) Hydrothermal oxidation in the Biwabik iron formation, Minnesota, USA. Miner Deposita 53: 1143-1166

Machamer JF, Tolbert GE, L'Esperance RL (1991) The discovery of Serra dos Carajas. Econ Geol Monograph 8, pp. 275-285

MacPhail MK, Stone MS (2004) Age and palaeoenvironmental constraints on the genesis of the Yandi channel iron deposits, Marillana Formation, Pilbara, northwestern Australia. Aust J Earth Sci 51: 497-520

Marsden RW (1968) Geology of the iron ores of the Lake Superior region in the United States. In: Ore deposits of the United States, 1933-1967, Graton-Sales Vol. 1, pp. 489-506. New York, Am Inst Min Metall Petrol Engineers

Maynard JB (2010) The chemistry of manganese ores through time: A signal of increasing diversity of Earth-surface environments. Econ Geol 105: 535-552

McIntosh JL, Farag JS, Slee KJ (1975) Groote Eylandt manganese deposits. In: Knight CL (ed) Economic geology of Australia and Papua New Guinea, 1. Metals, pp. 815-821. Melbourne, Australasian Inst Min Metall, Monograph 5.

Morey GB (1999) High-grade iron ore deposits of the Mesabi Range, Minnesota – Product of a continental-scale Proterozoic ground-water flow system. Econ Geol 94: 133-142

Morey GB, Southwick DL (1993) Stratigraphic and sedimentological factors controlling the distribution of epigenetic manganese deposits in iron-formation of the Emily district, Cuyuna Iron Range, east-central Minnesota. Econ Geol 88: 104-122

Morey GB, Southwick DL (1995) Allostratigraphic relationships of Early Proterozoic iron-formations in the Lake Superior region. Econ Geol 90: 1983-1993

Morris RC, Ramanaidou ER (2007) Genesis of the channel iron deposits (CID) of the Pilbara region, Western Australia. Aust J Earth Sci 54: 733-756

Mücke A (2006) Chamosite, siderite and the environmental conditions of their formation in chamosite-type Phanerozoic ooidal ironstones. Ore Geol Rev 28: 235-249

Mücke A, Farshad F (2005) Whole-rock and mineralogical composition of Phanerozoic ooidal ironstones: Comparison and differentiation of types and subtypes. Ore Geol Rev 26: 227-262

Parisot C, Schmit J-F (1994) Le fer – mémoire et reconversion. Guide d'excursion du Congrès Lorraine de l'APBG 1994.

Pracejus B, Bolton BR (1992) Geochemistry of supergene manganese oxide deposits, Groote Eylandt, Australia. Econ Geol 87: 1310-1335

Rasmussen B, Fletcher IR, Muhling JR, Thorne WS, Broadbent GC (2007) Prolonged history of episodic fluid flow in giant hematite ore bodies: Evidence from in situ U-Pb geochronology of hydrothermal xenotime. Earth Planet Sci Letters 258: 249-259

Ribeiro DT, Carvalho RM (2002) Simulation of weathered iron ore facies: Integrating leaching concepts and geostatistical model. In: Armstrong M, Bettini C, Champigny N, Galli A, Remacre A (eds) Geostatistics Rio 2000. Dordrecht, Kluwer, pp. 101-115

Rosière CA, Rios FJ (2004) The origin of hematite in high-grade iron ores based on infrared microscopy and fluid inclusion studies: the example of the Conceiçao mine, Quadrilátero Ferrífero, Brazil. Econ Geol 99: 611-624

Rosière CA, Spier CA, Rios FJ, Suchau VE (2008) The itabirite from the Quadrilátero Ferrífero and related high-grade ores: an overview. Reviews in Economic Geology, v. 15, pp. 223-254

Rosière CA, Heimann A, Oyhantçabal P, Santos JOS (2018) The iron formations of the South American platform. In: Siegesmund S, Basei MAS, Oyhantçabal P, Oriolo S (eds) Geology of southwest Gondwana, vol. 1, pp. 34-87. Heidelberg, Springer International

Roy S (2006) Sedimentary manganese metallogenesis in response to the evolution of the Earth system. Earth-Sci Rev 77: 273-305

Simpson TA, Gray TR (1968) The Birmingham Red-Ore district, Alabama. In: Ore deposits of the United States, 1933-1967, Graton-Sales Vol. 1, pp. 187-206. New York, Am Inst Min Metall Petrol Engineers

Spier CA, Barros de Oliveira SM, Rosiere CA (2003) Geology and geochemistry of the Aguas Claras and Pico iron mines, Quadrilatero Ferrifero, Minas Gerais, Brazil. Miner Deposita 38: 751-774

Spier CA, Barros de Oliveira SM, Rosiere CA, Ardisson JD (2008) Mineralogy and trace-element geochemistry of the high-grade iron ores of the Aguas Claras mine and comparison with the Capao Xavier and Tamandua iron ore deposits, Quadrilatero Ferrifero, Brazil. Miner Deposita 43: 229-254

Taner MF, Chemam M (2015) Algoma-type banded iron formation (BIF), Abitibi greenstone belt, Quebec, Canada. Ore Geol Rev 70: 31-46

Taylor D, Dalstra HJ, Harding AE, Broadbent GC, Barley ME (2001) Genesis of high-grade hematite orebodies of the Hamersley Province, Western Australia. Econ Geol 96: 837-873

Thorne WS, Hagemann SG, Barley M (2004) Petrographic and geochemical evidence for hydrothermal evolution of the North Deposit, Mt Tom Price, Western Australia. Miner Deposita 39: 766-783

Thorne W, Hagemann S, Vennemann T, Oliver N (2009) Oxygen isotope compositions of iron oxides from high-grade BIF-hosted iron ore deposits of the central Hamersley Province, Western Australia: Constraints on the evolution of hydrothermal fluids. Econ Geol 104: 1019-1035

Thorne WS, Hagemann SG, Sepe D, Dalstra HJ, Banks DA (2014) Structural control, hydrothermal alteration zonation, and fluid chemistry of the concealed, high-grade 4EE iron orebody at the Paraburdoo 4E deposit, Hamersley Province, Western Australia. Econ Geol 109: 1529-1562

Trendall AF, Blockley JG (1970) The iron formations of the Precambrian Hamersley Group, Western Australia. Geol Surv Western Australia Bulletin 119, 366 pp

Trendall AF, Nelson DR, deLaeter JR, Hassler SW (1998) Precise zircon U-Pb ages from the Marra Mamba iron formation and Wittenoom Formation, Hamersley Group, Western Australia. Aust J Earth Sci 45: 137-142

Tsikos H, Beukes NJ, Moore JM, Harris C (2003) Deposition, diagenesis, and secondary enrichment of metals in the Paleoproterozoic Hotazel Iron Formation, Kalahari Manganese Field, South Africa. Econ Geol 98: 1449-1462

Varentsov IM (1964) Sedimentary manganese ores. Elsevier, Amsterdam, 119 pp.

Varentsov IM, Rakhmanov VP (1974) Deposits of manganese. In: Smirnov VI (ed) Ore deposits of the USSR, Vol. 1 (English translation 1977), pp. 114-178. MIR Publishers, Moscow.

Walter R (1995) Geologie von Mitteleuropa. Schweizerbart'sche Verlagsbuchhandlung, Stuttgart, 566 pp